



# Insights into the CO-mediated deactivation mechanism for dimethyl ether carbonylation reaction over a H-MOR catalyst

Mingguan Xie<sup>a,b</sup>, Xudong Fang<sup>a</sup>, Zhiyang Chen<sup>a</sup>, Hongchao Liu<sup>a,\*</sup>, Bin Li<sup>a,b</sup>, Leilei Yang<sup>a,b</sup>, Cheng Li<sup>a,b</sup>, Wenliang Zhu<sup>a,\*</sup>

<sup>a</sup> National Engineering Research Center of Lower-Carbon Catalysis Technology, Dalian Institute of Chemical Physics, Chinese Academy of Sciences, Dalian, Liaoning 116023, China

<sup>b</sup> University of Chinese Academy of Sciences, Beijing 100049, China

## ARTICLE INFO

### Keywords:

DME carbonylation  
Mordenite  
Deactivation  
CO  
Methyl cyclopentenone

## ABSTRACT

Dimethyl ether (DME) carbonylation to methyl acetate (MAc) catalyzed by H-MOR catalyst has aroused wide interest due to its high efficiency as an emerging method for ethanol production. However, the rapid deactivation of H-MOR catalyst results in great challenges for its industrial application, urging a clear understanding of the intricate carbonylation deactivation mechanism. Herein, we discover a CO-mediated deactivation mechanism over H-MOR catalyst, which is beyond the traditional understanding that deactivation is originated from DME/methanol-to-hydrocarbon (DTH/MTH) chemistry. It is revealed that the coupling reaction of CO or MAc with olefins accelerate the catalyst deactivation, and methyl cyclopentenones (MCPOs) are first identified as the key intermediates for aromatic cokes formation over H-MOR catalyst. A more comprehensive mechanism for DME carbonylation deactivation is proposed based on the understanding. This study would provide valuable insights into understanding the carbonylation process and offer potential directions for developing carbonylation catalysts with enhanced stability.

## 1. Introduction

Ethanol, a significant renewable green energy, can be used as an environmentally friendly gasoline additive or a raw material to produce various chemical products [1,2]. Dimethyl ether (DME) carbonylation to methyl acetate (MAc) is of great significance as an essential step to produce the green fuel ethanol from syngas [3,4], which has attracted widespread attention. Since the groundbreaking utilization of zeolite-catalyzed DME carbonylation reactions [5,6], much effort has been undertaken, including reaction mechanism [7–12], zeolite synthesis and modification [13–19]. H-MOR zeolite exhibits the highest carbonylation activity due to its unique Brønsted acid sites (BAS) in eight-membered ring (8-MR) side pocket among the acidic zeolites investigated, [7–9,19]. However, it suffers from rapid deactivation due to the accumulation of coke within 12-MR pores during carbonylation reaction, presenting a substantial challenge to its large-scale application.

In order to develop a stable H-MOR catalyst for DME carbonylation reaction, numerous studies have been carried out, especially on the deactivation mechanism of detrimental coke [11,20–23]. It's widely

acknowledged that 12-MR channel of MOR, with its acid sites and large voids, is beneficial for the formation of coke precursors. Furthermore, both DME and MAc are considered to induce cokes formation within the 12-MR channel [20–22]. Recent research has unveiled the synergistic effects of acid sites in the 8-MR and 12-MR channels of MOR during the formation of aromatic coke [11,23]. Specifically, ketenes, crucial intermediates generated during the carbonylation process, are formed in 8-MR BAS and then transformed into coke within 12-MR BAS. Despite some progress has been made in the influence of BAS distribution on coke formation, the evolution of coke during DME carbonylation reaction is still believed to share similarities with the DME/methanol-to-hydrocarbon (DTH/MTH) chemistry [11,20–27]. In this context, DME/MAc/ketene are converted into olefins and subsequently evolved into aromatic coke via hydrogen transfer reaction within 12-MR BAS. However, an obvious difference between DME carbonylation and DTH/MTH lies in the introduction of a substantial quantity of CO into the reaction system. Excessive CO exist during DME carbonylation reaction, which are reasonable to infer that CO plays an important role on the formation of coke specially for the

\* Corresponding authors.

E-mail addresses: [chliu@dicp.ac.cn](mailto:chliu@dicp.ac.cn) (H. Liu), [wzhu@dicp.ac.cn](mailto:wzhu@dicp.ac.cn) (W. Zhu).

<https://doi.org/10.1016/j.apcata.2024.119701>

Received 6 January 2024; Received in revised form 26 February 2024; Accepted 20 March 2024

Available online 21 March 2024

0926-860X/© 2024 Elsevier B.V. All rights reserved.

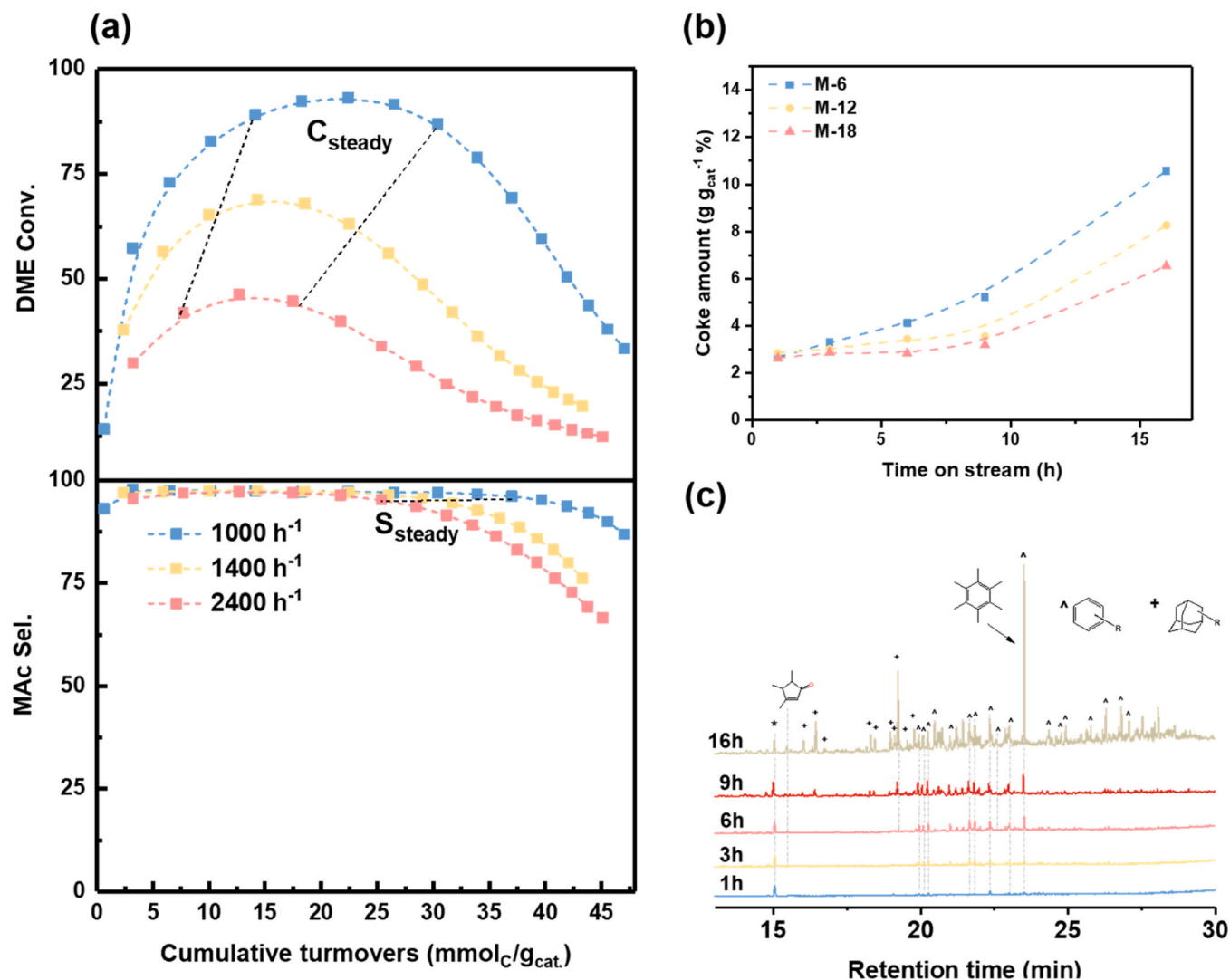


Fig. 1. The deactivation behaviors over H-MOR catalyst for DME carbonylation. (a) The catalytic performance at different gas hourly space velocity (GHSV). (b) TG analyses for coke amount at different time on stream (TOS) and different catalyst bed height at GHSV 2400 h<sup>-1</sup>. (c) GC-MS analyses for retained species after different TOS of M-6 at GHSV 2400 h<sup>-1</sup>. Reaction condition: 473 K, 2 MPa,  $n_{\text{DME}}/n_{\text{CO}}/n_{\text{H}_2} = 5/35/60$ . GHSV is labeled in the picture. The steady state of conversion and selectivity is denoted as  $C_{\text{steady}}$  and  $S_{\text{steady}}$ . The internal standard peak C<sub>2</sub>Cl<sub>6</sub> (10 ppm) was indicated by \* in the chromatograms.

aromatics-based deactivation species [28,29]. It has been reported that CO could accelerate coke formation by kinetic studies [23,30]. Unfortunately, few investigations focus on how CO participate in the formation of the coke species and modulate the deactivation reaction network [23]. Recently, we reported a cyclic oxygenates-based deactivation mechanism for DME carbonylation over a H-MOR-py catalysts [31]. Specifically, the excessive acetyl groups produced by CO are converted to ketenes in 8-MR side pockets and then transformed into cyclic oxygenates in 12-MR. Nonetheless, the cyclic oxygenates is difficult to be observed over H-MOR with the BASs in the 8-MR and 12-MR channel, indicating that the more complicate deactivation network must be existed. Consequently, in-depth understanding of the role of CO on the deactivation mechanism is crucial for designing new catalysts and promoting catalytic performance towards the DME carbonylation reaction, but it remains challenging due to the complexity of the deactivation network.

Here, we present a CO-mediated deactivation mechanism for DME carbonylation over H-MOR catalyst. It is demonstrated that CO could facilitate the formation of aromatic cokes through a coupling reaction involving either itself or MAC with olefins using various characterizations including gas chromatography-mass spectrometry (GC-MS), in situ

Ultraviolet-Visible diffuse reflectance spectrum (UV-Vis DRS), in situ diffuse reflectance infrared Fourier transform (DRIFT), <sup>13</sup>C isotope test and probe tests. Methyl cyclopentenones (MCPOs) originating from CO are first captured and proved to be the key precursor of aromatic cokes over H-MOR catalyst in the DME carbonylation reaction. This is distinct from the general cognition of the deactivation only caused by the DTH/MTH reaction. Based on the discovery, a more comprehensive deactivation roadmap is provided. This preliminary work would share an unusual perspective to understand the deactivation mechanism for small molecular conversion with CO in zeolites.

## 2. Experimental section

### 2.1. Catalyst preparation

MOR zeolite (Si/Al~12) was purchased from YanChang-ZhongKe Catalyst Ltd, the same as the catalyst used in previous research [31]. Typically, the purchased MOR is calcined to remove template at 823 K for 4 h. NH<sub>4</sub>-MOR was obtained by ion-exchanges with 1 mol/L NH<sub>4</sub>NO<sub>3</sub> solution (solution/zeolite mass ratio = 10) at 353 K for 1 h. The solution was filtered and washed with deionized water. This ion-exchange

procedure was repeated twice. After drying at 393 K overnight, the catalyst is calcined at 823 K for 4 h to obtain H-MOR.

## 2.2. Catalytic tests

The DME carbonylation reaction or experiments with different reactants or probe molecules were evaluated in a fixed bed reactor. Typically, the H-MOR catalyst (20–40 mesh) was pretreated with N<sub>2</sub> in the reactor at 553 K for 2 h, and then cooled to the reaction temperature. A mixture of reactant gas was introduced. The products were analyzed by an Agilent 7890 A gas chromatograph equipped with HP-PLOT Q capillary column and FID detector. In DME carbonylation, H-MOR catalysts were divided into three layers by quartz wool in a continuous flow fixed-bed stainless steel reactor. The reactant flow passes vertically through the catalyst from top to bottom, and the height of each catalyst bed is 6 mm. From top to bottom, each catalyst bed is denoted as the height starting from the start of catalyst bed: M-6, M-12, M-18, as shown in Figure S1. To suppress rapid deactivation of H-MOR catalyst, DME carbonylation is conducted in H<sub>2</sub> atmosphere to capture the potential intermediates [32,33]. The DME conversion and products selectivity were calculated on a molar carbon basis.

$$\text{Conv. (DME, \%)} = \frac{(\sum n \times C_{nH_mO_1} - 2 \times C_{\text{DME, outlet}})}{\sum n \times C_{nH_mO_1}} \times 100\%$$

$$\text{Sel. (C}_n\text{H}_m\text{O}_1, \%) = \frac{n \times C_{nH_mO_1}}{\sum n \times C_{nH_mO_1}} \times 100\%$$

where C<sub>nH<sub>m</sub>O<sub>1</sub></sub> represents the molar concentration of C<sub>nH<sub>m</sub>O<sub>1</sub></sub> and n is the number of carbons in C<sub>nH<sub>m</sub>O<sub>1</sub></sub>.

## 2.3. Catalysts characterization

An SDTQ600 instrument was utilized to perform thermal gravimetric (TGA) analysis. The instrument was setup at the temperature range of 323 – 1173 K with a heating rate of 10 K/min under an air flow of 100 mL min<sup>-1</sup>. Coke content is defined as the amount of carbonaceous components in the calcined catalyst per unit mass, and mass loss between 573 – 1173 K measured by TGA is used to estimate coke content.

The organic species retained in the spent H-MOR catalysts were analyzed by the method of Guisnet [34]. 50 mg of the spent H-MOR catalysts were dissolved in a 1 mL 20 wt% HF solution. After neutralized by a 5 wt% NaOH solution, the soluble organics were extracted by 2 mL CH<sub>2</sub>Cl<sub>2</sub> which contains 10 ppm C<sub>2</sub>Cl<sub>6</sub> as an internal standard, and then analyzed via an Agilent 7890B GC-MS instrument which was equipped with an HP-5 capillary column. All organics inside the spent catalyst in this experiment is soluble by CH<sub>2</sub>Cl<sub>2</sub> and no organic species is observed in the water phase (Figure S2).

In situ UV-vis DRS were recorded in the diffuse mode on the Cary 5000 spectrometer with the wavenumber range from 200 to 800 nm and scanning speed at 300 nm/min. H-MOR catalyst powder was loaded into the diffuse reflectance cell and calcined at 573 K for 30 min with flowing N<sub>2</sub>. After cooling to the 423 K, the cofeed of 1DME /49 N<sub>2</sub> or 1DME /49CO were introduced into the cell, and in situ UV-vis DRS were collected with increasing temperature from 423 K to 523 K. All the UV-vis DRS were obtained by subtracting the spectra of the H-MOR zeolite framework from the collected spectra at the corresponding temperatures.

In-situ DRIFT Spectra was carried out on a Bruker Tensor 27 instrument equipped with a diffuse reflectance attachment and MCT detector. H-MOR samples was placed in the diffuse reflectance infrared cell and heated to 573 K for 60 min with flowing N<sub>2</sub>. After cooling to the 473 K, 1DME/49 N<sub>2</sub> was first introduced into the cell for 100 min, and then 1DME/49CO was introduced into the cell for 90 min. The spectra were scanned by collecting 32 scans at 4 cm<sup>-1</sup> continuously to observe surface species. All the DRIFT spectra were obtained by subtracting the

spectra of the H-MOR zeolite framework from the collected spectra.

<sup>13</sup>C isotope tracing experiments was carried out in a fixed bed reactor. Typically, the H-MOR catalyst (20–40 mesh) was pretreated with N<sub>2</sub> in the reactor at 553 K for 2 h, and then cooled to 473 K. A mixture of CO and DME was introduced into reactor in the presence of <sup>13</sup>CO or <sup>12</sup>CO. The catalysts were collected, treated following Guisnet's method and analyzed by GC-MS and <sup>13</sup>C liquid-state NMR. The <sup>13</sup>C NMR spectra of catalyst were collected on a Bruker Avance III 700 MHz spectrometer.

## 3. Results and discussion

### 3.1. Deactivation behaviors of H-MOR in DME carbonylation

H-MOR (Si/Al ca. 12), used in our previous research [31], was employed as catalyst, which were divided into three layers by quartz wool in a continuous flow fixed-bed stainless steel reactor. The DME carbonylation reaction was conducted with different gas hourly space velocities (GHSV) on the H-MOR catalyst at 473 K and 2 MPa, as shown in Fig. 1. With the time proceeding, the DME conversion gradually increased and maintained a steady state for a short time at a constant GHSV. As GHSV increased from 1000 h<sup>-1</sup> to 2400 h<sup>-1</sup>, the time of steady state declined from 5 h to 3 h and the MAc selectivity decrease more rapidly, suggesting a more rapid deactivation. Additionally, Figure S1 showed that the hydrocarbons (CH<sub>x</sub>) and methanol selectivity obviously increased after a short steady state, which the higher the GHSV, the higher the selectivity to CH<sub>x</sub> and methanol. Moreover, the amount of aromatic carbon deposit increased with increasing GHSV (Figure S3), suggesting a more easily formation of aromatic deposit in the high GHSV. Therefore, these observations can be deduced that a higher GHSV is detrimental to catalyst stability due to the formation of a large number of aromatic species. It is known that a higher the GHSV means the shorter the residence time. The rapid formation of aromatic deposits may be due to the catalyst being exposed to more reactants in a short residence time, producing a large number of aromatic deposit precursors.

Furthermore, the spatiotemporal distribution and evolution of retained species over the spent catalysts were investigated. Fig. 1b showed that the coke amount over the spent catalysts in the different catalyst bed height changes with time under conditions of 473 K, 2.0 MPa and 2400 h<sup>-1</sup>. Specifically, only small amount of coke could be detected on different catalyst bed height within 3 h. However, an obvious increase in the amount of coke was observed after 6 h, particularly in the front of the catalyst bed. As shown in Fig. 1c and Figure S4, the retained species in the spent catalyst collected in the 0–6 mm (M-6) were analyzed by GC-MS. The retained species mainly involved polymethyl benzene, adamantane and methyl cyclopentadiene, which increased gradually with time particular after 6 h. Thereinto, the adamantane, as a typical coke precursor in MTH/DTH reaction [35,36], existed after 6 h. At the same time, the DME conversion has decreased and the content of aromatic species increased. Consequently, it can be concluded that the above retained species play an important role in catalyst deactivation. These observations seemed to reveal that the deactivation process in DME carbonylation reaction is similar with that in MTH/DTH reaction. Specifically, aromatics were generated from olefins via hydrogen transfer reactions with methyl cyclopentadienyl cations as intermediate in the traditional DTH/MTH reaction [25–27]. Nonetheless, a small amount of MCPO was detected for the first time in DME carbonylation, which also was observed in different catalyst bed height (Figure S5). Moreover, the content of methyl cyclopentenone and aromatics also exhibited a positive correlation. Therefore, we speculated that there were another deactivation pathways reaction with oxygenates as the intermediate similar with that catalyzed by H-MOR-py. Remarkably, cyclic oxygenates emerged as the primary deactivated species in DME carbonylation reaction catalyzed by H-MOR-py [31]. Conversely, aromatics species were the main deactivated species when H-MOR was

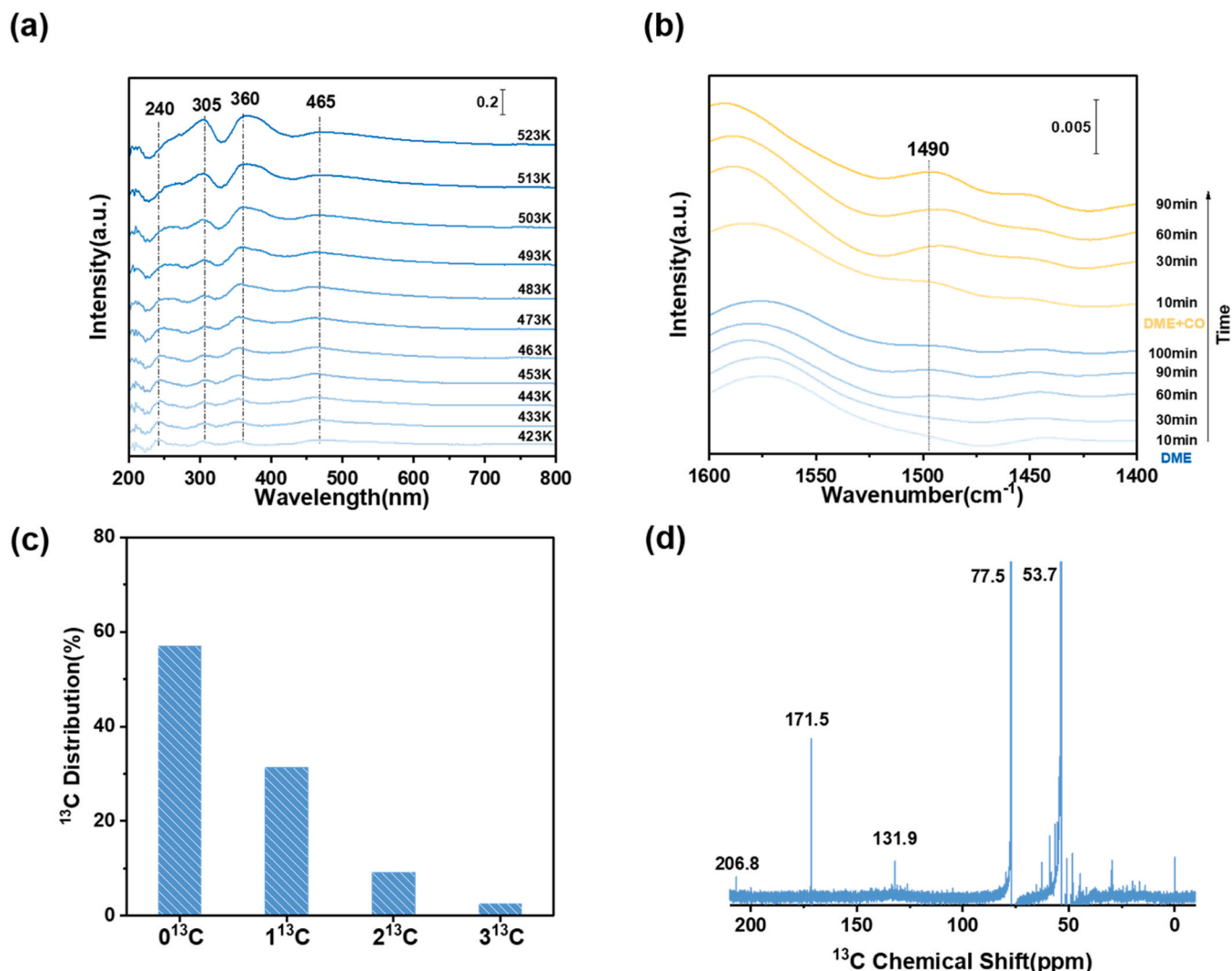


**Fig. 2.** Characterization to prove the CO role in aromatics retained in the spent H-MOR catalyst. (a) In situ UV-vis spectra recorded during the reaction of DME and CO with increasing temperature from 423 K to 523 K. (b) In situ DRIFT spectra recorded in the coke region during the reaction of DME alone for 100 min and then the reaction of DME and CO for 90 min. (c)  $^{13}\text{C}$  distribution of the hexamethylbenzene GC-MS analyses for retained species in the spent catalyst after  $^{13}\text{C}$  isotope test. (d)  $^{13}\text{C}$  liquid-state MAS NMR spectroscopy of the retained species in the spent catalyst after  $^{13}\text{C}$  isotope test. 53.7 ppm is assigned to  $\text{CH}_2\text{Cl}_2$ ; 77.5 ppm is  $\text{CDCl}_3$ ; 171.5 ppm is unsaturated C atom of MAC. Reaction condition: (a) 0.1 MPa,  $n_{\text{DME}}/n_{\text{CO}} = 1/49$ . (b) 473 K, 0.1 MPa, DME:  $n_{\text{DME}}/n_{\text{N}_2} = 1/49$ ; DME+CO:  $n_{\text{DME}}/n_{\text{CO}} = 1/49$ . (c), (d) 473 K, 0.5 MPa,  $n_{\text{DME}}/n_{\text{CO}} = 1/49$ , GHSV =  $3000 \text{ h}^{-1}$ .

used as a catalyst. The apparent difference might be caused by the distinct acid distribution, which also indicated that a more intricate deactivation mechanism is present over H-MOR due to the complex distribution of BASs in the different channel.

### 3.2. Deactivation mechanism of H-MOR in DME carbonylation

To clarify the deactivation mechanism during the DME carbonylation reaction catalyzed by H-MOR, in situ UV-vis DRS and in situ DRIFT experiments were conducted under different conditions. Figure S6 showed the evolution of intermediate over H-MOR for the DME conversion in  $\text{N}_2$  atmosphere. The peaks at ca. 360 nm and 465 nm [37–39], which were assigned to polymethyl benzene and polymethyl naphthalene, respectively, appeared and then increased with temperature. These changes were agreement with the traditional deactivation mechanism same as the MTH/DTH reaction. Notably, Fig. 2a illustrated that the new peak at ca. 240 nm, attributed to unsaturated aldehydes/ketones [37], appeared and gradually increased in the range of 423 K ~ 463 K in CO atmosphere, which might be formed by MCPOs. However, the peak decreased gradually and vanished with increasing temperature. These

observations suggested that MCPOs can be formed and then converted during the DME carbonylation over H-MOR. Therefore, we inferred that MCPOs might be an important coke precursor resulting from the existence of CO. To further verify the role of CO, in situ DRIFT experiments were performed for the conversion of DME in  $\text{N}_2$  or CO atmosphere over H-MOR at 473 K, as shown in Fig. 2b. According to the previous work [23], the peak at  $1490 \text{ cm}^{-1}$  was assigned to the  $\text{C}=\text{C}$  of aromatics. In the  $\text{N}_2$  atmosphere, the peak at  $1490 \text{ cm}^{-1}$  appeared and changed slightly with time prolonged. Obviously, the growth of the peak at  $1490 \text{ cm}^{-1}$  was more rapid during the DME carbonylation reaction. These results indicated that CO participate in and accelerated the formation of aromatics.

To directly confirm the role of CO in the formation of aromatic deposition, a  $^{13}\text{C}$  isotope test was conducted. Fig. 2c exhibited the  $^{13}\text{C}$  distribution of hexamethylbenzene, a main aromatic species analyzed by GC-MS (Figure S7). It can be observed that hexamethylbenzene contained a content of  $^{13}\text{C}$  atoms, suggesting the participation of CO into these species. As shown in Figure S7, MCPOs were also detected in the spent catalyst. Furthermore, the mass fragment of MCPOs and hexamethylbenzene shifted towards larger masses (Figure S8), further

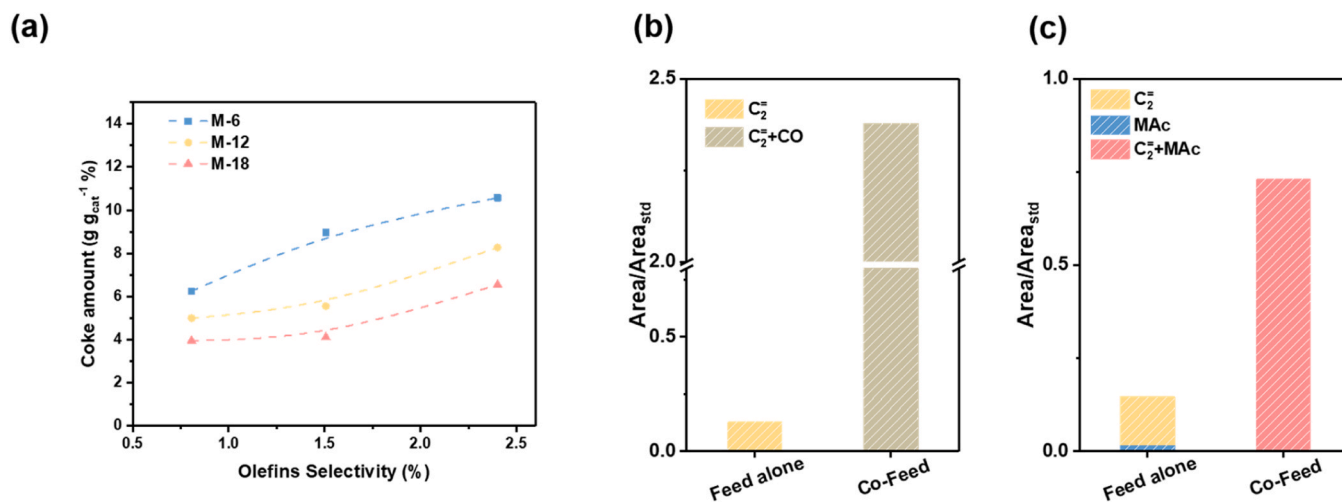


**Fig. 3.** Characterization to prove the olefins involve in aromatics retained in the spent H-MOR catalyst. (a) relationship between olefins selectivity at different GHSV in Fig. 1a and the coke amount in the spent catalyst. (b), (c) The amount of hexamethylbenzene in the spent catalyst after the reaction with different reactant. Reaction condition: (b), (c) 463 K, 2 MPa, GHSV = 24000 h<sup>-1</sup>, Ar as balance gas. MAc: 12.3 kPa MAc; C<sub>2</sub>: 2.48kPa ethylene; C<sub>2</sub> + MAc: 2.48kPa ethylene, 12.3 kPa MAc; C<sub>2</sub> + CO: 2.48kPa ethylene, 172.8 kPa CO.

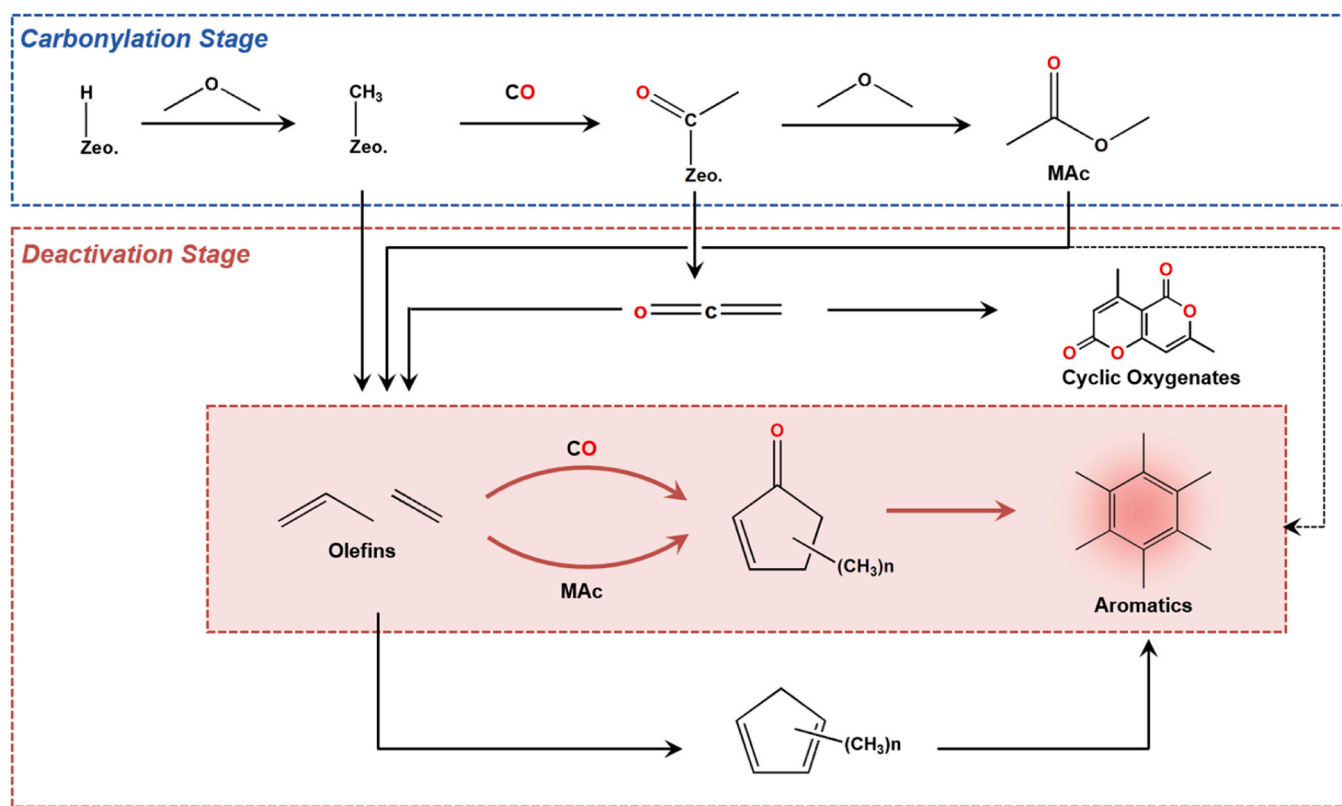


**Fig. 4.** The deactivation mechanism proposed for DME carbonylation in H-MOR catalyst.

suggesting the participation of CO into these species. To further correlate the relationship between MCPOs and aromatic cokes, the retained species were analyzed by <sup>13</sup>C MAS NMR. Fig. 2d exhibited obvious peaks at 131.9 ppm and 206.5 ppm, corresponding to the carbon atoms in the aromatic ring and the carbonyl of cyclopentenone [29]. Furthermore, aromatics are also detected when MCPO was introduced into the spent H-MOR catalyst (Figure S9), which directly demonstrated that MCPOs can be converted to aromatics species. In summary, these above findings collectively confirm the involvement of CO in the formation of aromatics via MCPO intermediate, further suggesting that the deactivation

mechanism during carbonylation reactions differs significantly from that of traditional DTH/MTH chemistry.

To further clarify the conversion of CO to aromatic coke, probe tests were conducted. It is known that CO alone cannot be converted in the H-type zeolite [23], implying that there should be a coupling reaction of CO and other reactants. Notably, the selectivity to olefins and the amount of coke exhibited a positive relationship in different GHSV (Fig. 3a), indicating that the olefins were closely related to the formation of coke. Ethylene, the most detected olefin during carbonylation (Figure S10), was employed as a probe molecule here. Obviously, the

amount of hexamethylbenzenes with ethylene as feeding alone was less than that in CO atmosphere (Fig. 3b). Additionally, more aromatic species were observed when MAc and ethylene were co-fed compared to when they were fed alone (Fig. 3c). These indicate that aromatic species can be induced by olefins or MAc in H-MOR catalyst. More importantly, beside the reaction of olefins or MAc itself, the coupling reaction between ethylene and CO/MAc promotes aromatics deposit formation.

Based on the results above and previous research, we constructed a route map for the reaction and deactivation network of DME carbonylation over H-MOR, as shown in Fig. 4. With regard to the deactivation network, there are three different ways. 1. Surface acetyl groups are converted to ketenes [10,11,21,27,31], and subsequently to deactivated cyclic oxygenates by polymerization and decarbonylation. 2. Some olefins produced on H-MOR catalyst during the reaction are converted to aromatics cokes via methyl cyclopentadienes intermediates, analogous to DTH/MTH chemistry. 3. Certain olefins can be coupled with CO or MAc to form MCPOs intermediates on H-MOR catalyst, which are then converted to aromatics cokes. The latter route is distinct from the conventional cognition about the deactivation and cannot be readily discerned due to the complexity of the deactivation network.

#### 4. Conclusion

In conclusion, we have successfully demonstrated that there is a deactivation route induced by CO among the complex deactivation networks over H-MOR for DME carbonylation. For the first time, we have illustrated the whole process of the deactivation induced by CO using various characterization analysis including GC-MS, in situ UV-vis DRS, in situ DRIFT,  $^{13}\text{C}$  isotope test and probe tests. The olefins produced from DME, MAc or ketene are coupled with CO or MAc over H-MOR catalyst to generate MCPOs intermediates. These MCPOs are easily converted to aromatic cokes, accelerating the deactivation of the carbonylation reaction. Consequently, we provide a more comprehensive roadmap for the DME carbonylation deactivation over H-MOR catalyst. These might provide valuable insights into the understanding of intricate reaction networks involved in DME carbonylation reaction.

#### CRediT authorship contribution statement

**Cheng Li:** Investigation. **Leilei Yang:** Investigation. **Bin Li:** Investigation. **Hongchao Liu:** Writing – review & editing, Visualization, Supervision, Investigation. **Zhiyang Chen:** Validation, Investigation. **Xudong Fang:** Writing – review & editing, Visualization, Investigation. **Mingguan Xie:** Writing – original draft, Visualization, Validation, Investigation. **Wenliang Zhu:** Writing – review & editing, Supervision.

#### Declaration of Competing Interest

The authors declare that they have no known competing financial interests or personal relationships that could have appeared to influence the work reported in this paper.

#### Data availability

Data will be made available on request.

#### Acknowledgements

We acknowledge the financial support from the National Natural Science Foundation of China (Grant Nos. 21972141, 21991094 and 21991090), the “Transformational Technologies for Clean Energy and Demonstration”, Strategic Priority Research Program of the Chinese Academy of Sciences (Grant No. XDA21030100), the Dalian High Level Talent Innovation Support Program (2017RD07), and the National Special Support Program for High Level Talents (SQ2019RA2TST0016). We acknowledge Mrs. Yanli He and Mr. Yijun Zheng for their help in the

characterization.

#### Appendix A. Supporting information

Supplementary data associated with this article can be found in the online version at doi:10.1016/j.apcata.2024.119701.

#### References

- [1] A.E. Farrell, R.J. Plevin, B.T. Turner, A.D. Jones, M. O'Hare, D.M. Kammen, Ethanol can contribute to energy and environmental goals, *Science* **311** (5760) (2006) 506–508.
- [2] M. Ni, D.Y.C. Leung, M.K.H. Leung, A review on reforming bio-ethanol for hydrogen production, *Int. J. Hydrog. Energy* **32** (15) (2007) 3238–3247.
- [3] G. Liu, G. Yang, X. Peng, J. Wu, N. Tsubaki, Recent advances in the routes and catalysts for ethanol synthesis from syngas, *Chem. Soc. Rev.* **51** (13) (2022) 5606–5659.
- [4] P. Lu, Q. Chen, G. Yang, L. Tan, X. Feng, J. Yao, Y. Yoneyama, N. Tsubaki, Space-Confinement Self-Regulation Mechanism from a Capsule Catalyst to Realize an Ethanol Direct Synthesis Strategy, *ACS Catal.* **10** (2) (2020) 1366–1374.
- [5] K. Fujimoto, T. Shikada, K. Omata, H.-o Tominaga, Vapor phase carbonylation of methanol with solid acid catalysts, *Chem. Lett.* **13** (12) (1984) 2047–2050.
- [6] P. Cheung, A. Bhan, G.J. Sunley, E. Iglesia, Selective carbonylation of dimethyl ether to methyl acetate catalyzed by acidic zeolites, *Angew. Chem. Int. Ed.* **45** (10) (2006) 1617–1620.
- [7] M. Boronat, C. Martínez-Sánchez, D. Law, A. Corma, Enzyme-like Specificity in Zeolites: A Unique Site Position in Mordenite for Selective Carbonylation of Methanol and Dimethyl Ether with CO, *J. Am. Chem. Soc.* **130** (48) (2008) 16316–16323.
- [8] P. Cheung, A. Bhan, G.J. Sunley, D.J. Law, E. Iglesia, Site requirements and elementary steps in dimethyl ether carbonylation catalyzed by acidic zeolites, *J. Catal.* **245** (1) (2007) 110–123.
- [9] A. Bhan, A.D. Allian, G.J. Sunley, D.J. Law, E. Iglesia, Specificity of Sites within Eight-Membered Ring Zeolite Channels for Carbonylation of Methyls to Acetyls, *J. Am. Chem. Soc.* **129** (16) (2007) 4919–4924.
- [10] D.B. Rasmussen, J.M. Christensen, B. Temel, F. Studt, P.G. Moses, J. Rossmeisl, A. Riisager, A.D. Jensen, Ketene as a Reaction Intermediate in the Carbonylation of Dimethyl Ether to Methyl Acetate over Mordenite, *Angew. Chem. Int. Ed.* **54** (25) (2015) 7261–7264.
- [11] W. Chen, G. Li, X. Yi, S.J. Day, K.A. Tarach, Z. Liu, S.-B. Liu, S.C. Edman Tsang, K. Góra-Marek, A. Zheng, Molecular Understanding of the Catalytic Consequence of Ketene Intermediates under Confinement, *J. Am. Chem. Soc.* **143** (37) (2021) 15440–15452.
- [12] W. Chen, K.A. Tarach, X. Yi, Z. Liu, X. Tang, K. Góra-Marek, A. Zheng, Charge-separation driven mechanism via acylium ion intermediate migration during catalytic carbonylation in mordenite zeolite, *Nat. Commun.* **13** (1) (2022). No. 7106.
- [13] Z. Xiong, E. Zhan, M. Li, W. Shen, DME carbonylation over a HSUZ-4 zeolite, *Chem. Commun.* **56** (23) (2020) 3401–3404.
- [14] X. Feng, J. Yao, H. Li, Y. Fang, Y. Yoneyama, G. Yang, N. Tsubaki, A brand new zeolite catalyst for carbonylation reaction, *Chem. Commun.* **55** (8) (2019) 1048–1051.
- [15] S.Y. Park, C.-H. Shin, J.W. Bae, Selective carbonylation of dimethyl ether to methyl acetate on Ferrierite, *Catal. Commun.* **75** (2016) 28–31.
- [16] M. Lusardi, T.T. Chen, M. Kale, J.H. Kang, M. Neurock, M.E. Davis, Carbonylation of Dimethyl Ether to Methyl Acetate over SSZ-13, *ACS Catal.* **10** (1) (2020) 842–851.
- [17] K. Cao, D. Fan, M. Gao, B. Fan, N. Chen, L. Wang, P. Tian, Z. Liu, Recognizing the Important Role of Surface Barriers in MOR Zeolite Catalyzed DME Carbonylation Reaction, *ACS Catal.* **12** (1) (2022) 1–7.
- [18] N. Chen, J. Zhang, Y. Gu, W. Zhang, K. Cao, W. Cui, S. Xu, D. Fan, P. Tian, Z. Liu, Designed synthesis of MOR zeolites using gemini-type bis(methylpyrrolidinium) dications as structure directing agents and their DME carbonylation performance, *J. Mater. Chem. A* **10** (15) (2022) 8334–8343.
- [19] Z. Xiong, G. Qi, E. Zhan, Y. Chu, J. Xu, J. Wei, N. Ta, A. Hao, Y. Zhou, F. Deng, et al., Experimental identification of the active sites over a plate-like mordenite for the carbonylation of dimethyl ether, *Chem* **9** (2023) 76–92.
- [20] H. Zhou, W. Zhu, L. Shi, H. Liu, S. Liu, Y. Ni, Y. Liu, Y. He, S. Xu, L. Li, et al., In situ DRIFT study of dimethyl ether carbonylation to methyl acetate on H-mordenite, *J. Mol. Catal. A: Chem.* **417** (2016) 1–9.
- [21] X. Wang, R. Li, C. Yu, Y. Liu, C. Xu, C. Lu, Study on the deactivation process of dimethyl ether carbonylation reaction over Mordenite catalyst, *Fuel* **286** (2021) 119480.
- [22] B. Li, J. Xu, B. Han, X. Wang, G. Qi, Z. Zhang, C. Wang, F. Deng, Insight into Dimethyl Ether Carbonylation Reaction over Mordenite Zeolite from in-Situ Solid-State NMR Spectroscopy, *J. Phys. Chem. C* **117** (11) (2013) 5840–5847.
- [23] Z. Cheng, S. Huang, Y. Li, K. Cai, Y. Wang, M.-y Wang, J. Lv, X. Ma, Role of Brønsted Acid Sites within 8-MR of Mordenite in the Deactivation Roadmap for Dimethyl Ether Carbonylation, *ACS Catal.* **11** (9) (2021) 5647–5657.
- [24] A.A.C. Reule, J.A. Sawada, N. Semagina, Effect of selective 4-membered ring dealumination on mordenite-catalyzed dimethyl ether carbonylation, *J. Catal.* **349** (2017) 98–109.

- [25] J. Li, Y. Wei, J. Chen, P. Tian, X. Su, S. Xu, Y. Qi, Q. Wang, Y. Zhou, Y. He, et al., Observation of Heptamethylbenzenium Cation over SAPO-Type Molecular Sieve DNL-6 under Real MTO Conversion Conditions, *J. Am. Chem. Soc.* **134** (2) (2012) 836–839.
- [26] S. Lin, Y. Zhi, W. Chen, H. Li, W. Zhang, C. Lou, X. Wu, S. Zeng, S. Xu, J. Xiao, et al., Molecular Routes of Dynamic Autocatalysis for Methanol-to-Hydrocarbons Reaction, *J. Am. Chem. Soc.* **143** (31) (2021) 12038–12052.
- [27] S. Müller, Y. Liu, F.M. Kirchberger, M. Tonigold, M. Sanchez-Sanchez, J.A. Lercher, Hydrogen Transfer Pathways during Zeolite Catalyzed Methanol Conversion to Hydrocarbons, *J. Am. Chem. Soc.* **138** (49) (2016) 15994–16003.
- [28] Z. Chen, Y. Ni, Y. Zhi, F. Wen, Z. Zhou, Y. Wei, W. Zhu, Z. Liu, Coupling of Methanol and Carbon Monoxide over H-ZSM-5 to Form Aromatics, *Angew. Chem. Int. Ed.* **57** (2018) 12549–12553.
- [29] X. Fang, H. Liu, Z. Chen, Z. Liu, X. Ding, Y. Ni, W. Zhu, Z. Liu, Highly Enhanced Aromatics Selectivity by Coupling of Chloromethane and Carbon Monoxide over H-ZSM-5, *Angew. Chem. Int. Ed.* **61** (13) (2022). No. e202114953.
- [30] Z. Cheng, S. Huang, Y. Li, J. Lv, K. Cai, X. Ma, Deactivation Kinetics for the Carbonylation of Dimethyl Ether to Methyl Acetate on H-MOR, *Ind. Eng. Chem. Res.* **56** (46) (2017) 13618–13627.
- [31] M. Xie, X. Fang, H. Liu, Z. Chen, B. Li, L. Yang, W. Zhu, Cyclic Oxygenate-Based Deactivation Mechanism in Dimethyl Ether Carbonylation Reaction over a Pyridine-Modified H-MOR Catalyst, *ACS Catal.* **13** (21) (2023) 14327–14333.
- [32] H. Xue, X. Huang, E. Ditzel, E. Zhan, M. Ma, W. Shen, Dimethyl Ether Carbonylation to Methyl Acetate over Nanosized Mordenites, *Ind. Eng. Chem. Res.* **52** (33) (2013) 11510–11515.
- [33] S. Arora, D. Nieskens, A. Malek, A. Bhan, Lifetime improvement in methanol-to-olefins catalysis over chabazite materials by high-pressure H<sub>2</sub> co-feeds, *Nat. Catal.* **1** (9) (2018) 666–672.
- [34] M. Guisnet, P. Magnoux, Coking and deactivation of zeolites – influence of the pore structure, *Appl. Catal.* **54** (1) (1989) 1–27.
- [35] Y. Wei, J. Li, C. Yuan, S. Xu, Y. Zhou, J. Chen, Q. Wang, Q. Zhang, Z. Liu, Generation of diamondoid hydrocarbons as confined compounds in SAPO-34 catalyst in the conversion of methanol, *Chem. Commun.* **48** (25) (2012) 3082–3084.
- [36] W. Zhang, S. Lin, Y. Wei, P. Tian, M. Ye, Z. Liu, Cavity-controlled methanol conversion over zeolite catalysts, *Nat. Sci. Rev.* **10** (9) (2023) nwad120.
- [37] C. Wei, J. Li, K. Yang, Q. Yu, S. Zeng, Z. Liu, Aromatization mechanism of coupling reaction of light alkanes with CO over acidic zeolites: Cyclopentenones as key intermediates, *Chem. Catal.* **1** (6) (2021) 1273–1290.
- [38] V. VanSpeybroeck, K. Hemelsoet, K. DeWispelaere, Q. Qian, J. VanderMynsbrugge, B. DeSterck, B.M. Weckhuysen, M. Waroquier, Mechanistic Studies on Chabazite-Type Methanol-to-Olefin Catalysts: Insights from Time-Resolved UV/Vis Microspectroscopy Combined with Theoretical Simulations, *ChemCatChem* **5** (1) (2013) 173–184.
- [39] K. Hemelsoet, Q. Qian, T. DeMeyer, K. DeWispelaere, B. DeSterck, B. M. Weckhuysen, M. Waroquier, V. VanSpeybroeck, Identification of Intermediates in Zeolite-Catalyzed Reactions by In Situ UV/Vis Microspectroscopy and a Complementary Set of Molecular Simulations, *Chem. Eur. J.* **19** (49) (2013) 16595–16606.